Acta Cryst. (1993). B49, 929–936

Structure Refinement of the Incommensurate Composite Crystal $Sr_{1.145}TiS_3$ Through the Rietveld Analysis Process

BY MITSUKO ONODA, MASANOBU SAEKI, AKIJI YAMAMOTO AND KATSUO KATO

National Institute for Research in Inorganic Materials, 1-1 *Namiki, Tsukuba, Ibaraki* 305, *Japan*

(*Received* 12 *December* 1992; *accepted* 25 *May* 1993)

Abstract

The structure of the incommensurate composite crystal of the trigonal sulfide $Sr_{1.145}TiS_3$, $M_r = 244.42$, has been analyzed on the basis of the four-dimensional superspace group P^{R3m}_{1s} using powder X-ray diffraction data and the Rietveld analysis process. The unit cell and other crystal data are $a_1 = a_2 = 11.5108\ (2)$, $a_3 = 2.99094\ (5)$ Å, $\sigma = [0\ 0\ 0.57227\ (2)]$, $V = 343.19$ Å^3, $D_x = 3.548$ Mg m^{-3} and $Z = 3$. R_{wp} was 0.104 on an incommensurate modulated structure model with 47 structural parameters. The crystal is composed of columns of face-shared polyhedra, $(TiS_{6/2})_\infty$, and rows of Sr, and both are parallel to the c axis.

Introduction

Only one paper has been published on the Sr—Ti—S system by Hahn & Mutschke (1956). They reported the powder X-ray diffraction pattern of the specimen synthesized at the composition of $SrTiS_3$, and they mentioned the possibility that the crystal structure of $SrTiS_3$ might be related to the $BaNiO_3$ type, although some reflection peaks of the powder X-ray diffraction pattern could not be indexed on the $BaNiO_3$-type unit cell. Recently, the existence of columnar composite crystals Sr_xTiS_3 ($1.05 \le x \le 1.22$) was revealed during our search in the Sr—Ti—S system, and the powder X-ray diffraction pattern was indexed in a four-dimensional formalism (Saeki & Onoda, 1993). As the composite crystal has, in general, an incommensurate modulated structure, the superspace-group theory (Janner & Janssen, 1980) should be applied to describe its structure. In this study the crystal structure of a composite crystal Sr_xTiS_3 ($x = 1.145$) was investigated through the superspace-group approach based on the powder X-ray diffraction data using the Rietveld analysis program *PREMOS* (Yamamoto, Takayama-Muromachi, Izumi, Ishigaki & Asano, 1992).

Experimental

The starting materials, $SrTiO_3$ (purity 99%) and $SrCO_3$ (99.9%), were mixed in proportion to Sr/Ti = 1.145 and heated in a furnace at 1073 K for 3 d in an atmosphere of CS_2 carried by N_2 gas. The specimen was then ground and heated again for 3 d at 1073 K in the same atmosphere. Lastly, the specimen was sealed in an evacuated silica tube and was heated for 2 d at 1173 K and then quenched in water. The X-ray and electron diffraction of the specimen was measured to obtain information on the crystal structure. The powder X-ray diffraction data* were collected with a step-scan procedure on a Philips PW1800-type diffractometer with an automatic divergence slit using Cu $K\alpha$ radiation. Conditions of measurement are listed in Table 1. Electron-diffraction patterns were taken from the crushed particles using a 400 kV electron microscope (JEOL 400 type).

Table 1. *Conditions of powder X-ray diffraction data collection*

Sample	Powder of synthesized $Sr_{1.145}TiS_3$
Instrument	Philips PW1800-type diffractometer
Radiation source	Cu $K\alpha_1$ and Cu $K\alpha_2$
Wavelengths (Å)	1.54060, 1.54439
Generator settings	40 kV, 50 mA
Step size (°), sample time (s)	0.020, 15.0
Monochromator	Counter-side graphite monochromator
Divergence slit	Automatic (irradiated sample length: 10.0 mm)
Range of 2θ (°)	5.00–100.00
Range of D spacing (Å)	1.00556–17.6596
Maximum intensity	37558 c.t.s., 2503.9 c.p.s.

Symmetry

As discussed in the previous paper (Saeki & Onoda, 1993), the strong reflections of the specimen could be indexed using two sets of hexagonal axes with common a and different c: for the TiS_3 part $a = 11.5108$ and $c_1 = 2.991$ Å; for the Sr part $a = 11.5108$ and $c_2 = 5.226$ Å. Four integers, h, k, l and m, are used as shown in Figs. 1 and 2 in order to index all reflections. Each reflection is expressed by $\mathbf{q} = h\mathbf{a}^* + k\mathbf{b}^* + l\mathbf{c}_1^* + m\mathbf{c}_2^*$, where $\mathbf{a}^*$ and $\mathbf{b}^*$ are the reciprocal vectors corresponding to $\mathbf{a}$ and $\mathbf{b}$. $\mathbf{c}_1^*$ and $\mathbf{c}_2^*$ are

* Raw powder X-ray diffraction data of $Sr_{1.145}TiS_3$ have been deposited with the British Library Document Supply Centre as Supplementary Publication No. SUP 71261 (20 pp.). Copies may be obtained through The Technical Editor, International Union of Crystallography, 5 Abbey Square, Chester CH1 2HU, England.

reciprocal to **c** for the TiS_3 and Sr parts respectively ($c_2^*/c_1^* = 0.57227$). The reciprocal vectors of the two subsystems are related to the minimal vector set in reciprocal space $\{\mathbf{a}_1^*, \mathbf{a}_2^*, \mathbf{a}_3^*, \mathbf{a}_4^*\} = \{\mathbf{a}^*, \mathbf{b}^*, \mathbf{c}_1^*, \mathbf{c}_2^*\}$ through the following Z matrices (Janner & Janssen, 1980).

Subsystem 1 (TiS_3)

$$Z^1 = \begin{pmatrix} 1 & 0 & 0 & 0 \\ 0 & 1 & 0 & 0 \\ 0 & 0 & 1 & 0 \end{pmatrix}$$

Subsystem 2 (Sr)

$$Z^2 = \begin{pmatrix} 1 & 0 & 0 & 0 \\ 0 & 1 & 0 & 0 \\ 0 & 0 & 0 & 1 \end{pmatrix}.$$

The cell constants in a four-dimensional formalism are $a_1 = a_2 = a = 11.5108$, $a_3 = c_1 = 2.991$ Å and $\sigma = (0\ 0\ 0.57227)$. Since the systematic reflection condition, $-h + k + l = 3n$ for $hkl0$, was observed in the electron and X-ray diffraction patterns, the possible space groups of the basic structure of the TiS_3 part

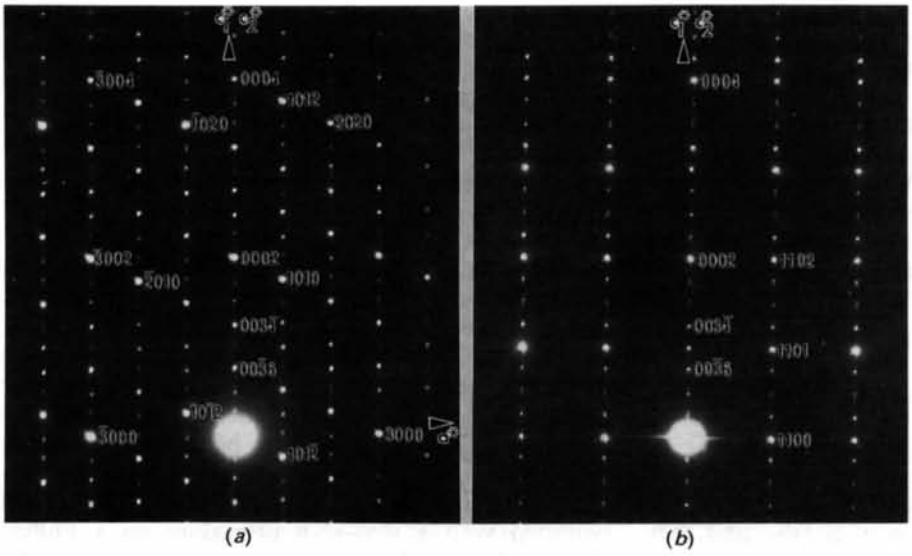

Fig. 1. Electron-diffraction patterns of $Sr_{1.145}TiS_3$ with incident beams parallel to (*a*) [010] and (*b*) [$\bar{1}$10] directions of the subsystems. The spots are indexed with four integers: *h*, *k*, *l* and *m*.

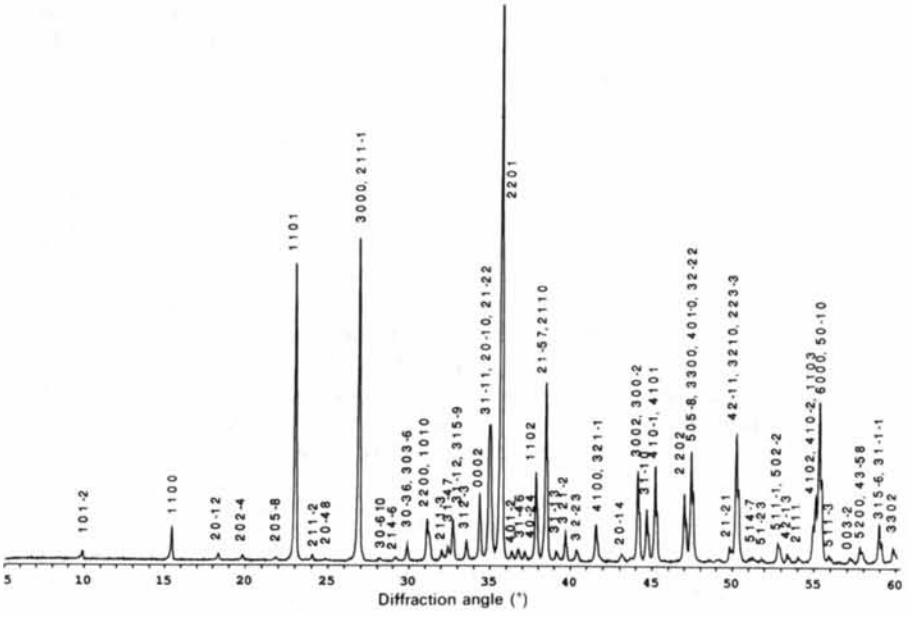

Fig. 2. The powder X-ray diffraction pattern of $Sr_{1.145}TiS_3$ measured by using Cu $K\alpha$ radiation and an automatic divergence slit. Reflections are assigned by four integers: *h*, *k*, *l* and *m*.

are considered to be $R\bar{3}m$ and $R3m$. For the main reflections of the Sr part, the conditions, $-h+k=3n$ for $hk0m$ and $m=2n$ for $(3j)00m$, were observed. These imply $P\bar{3}1c$ and $P31c$, because they become a simple condition $m=2n$ for $HH0m$ if the vectors $\mathbf{A}^*=2\mathbf{a}^*-\mathbf{b}^*$ and $\mathbf{B}^*=\mathbf{a}^*+\mathbf{b}^*$ are used. The possible superspace groups of the composite crystal could be determined from the space groups of the subsystems using the computer program *SGR*, and the results from the combination of $R3m$ and $P31c$ are shown in Table 2. The subsystem superspace groups for the first and second subsystem could be written as P^{R3m}_{1s} and R^{P31c}_{111}, and the modulation wavevectors selected for them were $\mathbf{c}_2^*$ and $\mathbf{c}_1^*$, respectively, based on the minimal-vector set.

The systematic reflection conditions were derived using the program *ASL*, and moreover the restriction conditions for the Fourier amplitudes of the modulation functions of atoms located at the special positions could be obtained through programs *SPA* (for scalar), *SPL* (for vector) and *SPT* (for tensor). It was confirmed that the observed extinction rules including satellite reflections are consistent with those calculated. The earlier versions of these programs are included in the supplementary materials of Kato & Onoda (1991*b*, 1992). In the program *PREMOS* the permutation matrix for the second subsystem $P^2=(3,4)$ is used instead of the Z matrices (Yamamoto, 1992).

Table 2. *Results of symmetry considerations*

(*a*) Generator set of symmetry operations

Space group		Superspace group
Subsystem 1	Subsystem 2	
(TiS_3 part)	(Sr part)	$[TiS_3]\,[2Sr]_{0.57227}$
$a=11.5108$	$a=11.5108=6.6460(3)^{1/2}$	$a=11.5108$
$c_1=2.9909$ Å	$c_2=5.226$ Å	$c=2.9909$ Å, $\sigma=(0\,0\,0.57227)$
$x+\frac{2}{3}, y+\frac{1}{3}, z+\frac{1}{3}$	$x+\frac{2}{3}, y+\frac{1}{3}, z$	$x_1+\frac{2}{3}, x_2+\frac{1}{3}, x_3+\frac{1}{3}, x_4$
$-y, x-y, z$	$-y, x-y, z$	$-x_2, x_1-x_2, x_3, x_4$
$-y, -x, z$	$-y, -x, z+\frac{1}{2}$	$-x_2, -x_1, x_3, x_4+\frac{1}{2}$
$[R3m]$	[extended $P31c$]	$[P^{R3m}_{1s}]$

(*b*) Systematic reflection conditions

Superspace group	Class			
	$hklm$	$h(-h)lm$	$h0lm$	$0klm$
P^{R3m}_{1s}	$-h+k+l=3n$	$m=2n$	$m=2n$	$m=2n$

(*c*) Requirements on the atomic modulation waves

A_i and B_i for $i=x, y, z$ and B are the cosine and sine amplitudes of the Fourier series.

Subsystem 1

Wavevector	Ti (0, 0, z)	S (x, $x/2$, z)
000 $(2n+1)$	$A_x=B_x=A_y=B_y=A_z=B_z=0$, $A_B=B_B=0$	$A_x=B_x=A_z=B_z=0$, $A_B=B_B=0$
000 $(2n)$	$A_x=B_x=A_y=B_y=0$	$A_x=2A_y$, $B_x=2B_y$

Subsystem 2

Wavevector	Sr ($\frac{1}{3}$, 0, z)
00 $(3n+1)0$	$A_x=\frac{1}{2}A_y+(3^{1/2}/2)B_y$, $B_x=-(3^{1/2}/2)A_y+\frac{1}{2}B_y$, $A_z=B_z=0$, $A_B=B_B=0$
00 $(3n+2)0$	$A_x=\frac{1}{2}A_y-(3^{1/2}/2)B_y$, $B_x=(3^{1/2}/2)A_y+\frac{1}{2}B_y$, $A_z=B_z=0$, $A_B=B_B=0$
00 $(3n)0$	$A_x=B_x=A_y=B_y=0$

(*d*) Superspace groups for the subsystems 1 and 2 used in the program *PREMOS*

Subsystem	1 (TiS_3 part)	2 (Sr part)
Generator set of the superspace group	$x+\frac{2}{3}, y+\frac{1}{3}, z+\frac{1}{3}, u$ $-y, x-y, z, u$ $-y, -x, z, u+\frac{1}{2}$	$x+\frac{2}{3}, y+\frac{1}{3}, z, u+\frac{1}{3}$ $-y, x-y, z, u$ $-y, -x, z+\frac{1}{2}, u$
Symbol	P^{R3m}_{1s}	R^{P31c}_{111}

Structure refinement

Refinement was performed on the basis of the powder X-ray diffraction data through a new version of the Rietveld analysis program *PREMOS* (Yamamoto, 1992). After several trials, a model was established employing the superspace groups P^{R3m}_{1s}: R^{P31c}_{111}. Values of scattering factors were taken from *International Tables for X-ray Crystallography* (1974, Vol. IV). Besides one scaling factor, atomic coordinates and isotropic thermal parameters, the Fourier

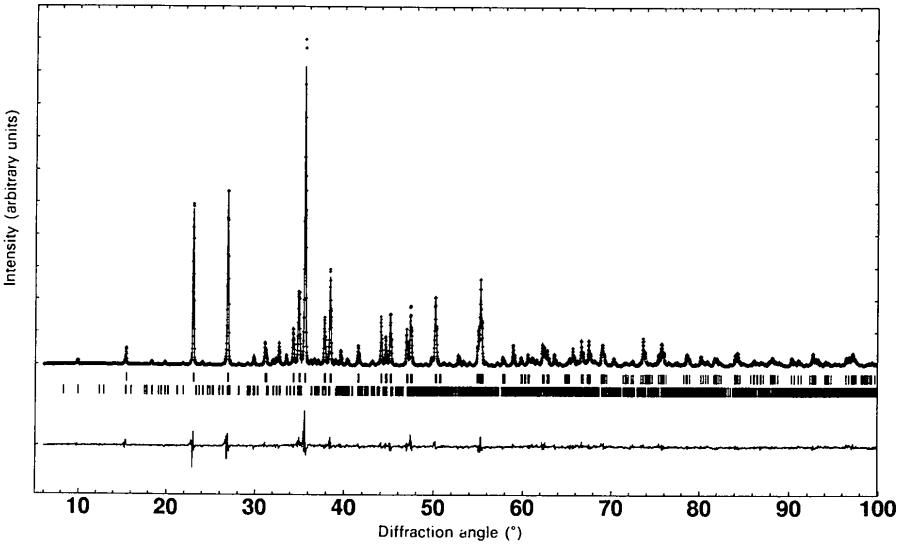

Fig. 3. The Rietveld analysis pattern of $Sr_{1.145}TiS_3$. The vertical bars below the diffraction pattern show the position of the main (upper) and satellite (lower) reflections of the two subsystems. The lower solid line represents the difference between the observed and calculated intensities.

amplitudes of the modulation functions which represent the deviation from the value in the fundamental structure were considered as structural parameters. As the atoms are located in special positions the modulation-function shapes are restricted as shown in Table 2(*c*). The region from $d =$ 11 to 1.0 Å of the powder X-ray diffraction pattern was used. As the satellite reflections (*hklm* with both *l* and *m* non-zero) up to the sixth order were observed in the pattern, the modulation waves up to the sixth order were considered. After preliminary refinement, the structure model was set up with displacive modulations for all atoms up to the sixth order and with modulations of isotropic thermal parameters up to the fourth order for S and up to the third order for Sr. The agreement was fairly good with 47 structural parameters; $R_{wp} = 0.104$, while those for the models with only displacive modulations up to the third and sixth order were respectively $R_{wp} = 0.141$ with 21 parameters and $R_{wp} =$ 0.109 with 41 parameters. The final profile fit and the difference pattern are shown in Fig. 3, and the final parameters are listed in Table 3.

Table 3. *Atomic parameters of* $Sr_{1.145}TiS_3$

The independent and propagated standard deviations are in parentheses and square brackets respectively. A_{hklm} and B_{hklm} are the amplitudes of the cosine and sine terms with wavevector $h\mathbf{a}^* + k\mathbf{b}^* + l\mathbf{c}_1^* + m\mathbf{c}_2^*$ in the modulation function expressed as a Fourier series. To obtain the parameter values for the average structure, the values of A_{0000} should be added to the corresponding fundamental values. If the average structure thus obtained is taken as the basic structure, the amplitudes of the higher ordered Fourier terms must be changed by compensating the phase difference corresponding to A_{0000}.

	x	*y*	*z*	*B* (Å²)
Subsystem 1				
Ti				
Fundamental	0.0	0.0	0.0	1.0
A_{0000}	0.0	0.0	0.0	0.37 (17)
A_{0002}	0.0	0.0	0.042 (12)	0.0
B_{0002}	0.0	0.0	0.058 (6)	0.0
A_{0004}	0.0	0.0	0.013 (10)	0.0
B_{0004}	0.0	0.0	−0.016 (10)	0.0
A_{0006}	0.0	0.0	0.009 (10)	0.0
B_{0006}	0.0	0.0	−0.018 (11)	0.0
S				
Fundamental	0.17	0.085	0.5	1.0
A_{0000}	−0.0099 (13)	−0.0050 [7]	0.027 (10)	0.4 (2)
A_{0001}	0.0	0.100 (4)	0.0	0.0
B_{0001}	0.0	−0.066 (4)	0.0	0.0
A_{0002}	0.0197 (19)	0.0099 [9]	−0.037 (9)	−1.6 (4)
B_{0002}	0.008 (3)	0.0041 [15]	−0.047 (6)	−0.4 (7)
A_{0003}	0.0	−0.009 (5)	0.0	0.0
B_{0003}	0.0	0.040 (2)	0.0	0.0
A_{0004}	−0.015 (2)	−0.0074 [11]	0.000 (5)	0.9 (6)
B_{0004}	−0.004 (3)	−0.0021 [17]	−0.002 (8)	−0.8 (6)
A_{0005}	0.0	−0.017 (6)	0.0	0.0
B_{0005}	0.0	−0.026 (4)	0.0	0.0
A_{0006}	0.015 (2)	0.0073 [12]	0.002 (10)	0.0
B_{0006}	0.003 (3)	0.001 [2]	0.027 (8)	0.0
Subsystem 2				
Sr				
Fundamental	0.33333	0.0	0.0	1.0
A_{0000}	0.0	0.0	−0.018 (8)	1.41 (13)
A_{0010}	0.0241 (6)	0.062 [19]	0.0	0.0
B_{0010}	−0.007 (2)	−0.0243 [12]	0.0	0.0
A_{0020}	−0.000 (2)	−0.0113 [12]	0.0	0.0
B_{0020}	0.0128 (6)	0.006 [2]	0.0	0.0
A_{0030}	0.0	0.0	0.018 (3)	1.3 (4)
B_{0030}	0.0	0.0	−0.008 (6)	−0.9 (4)
A_{0040}	−0.007 (2)	−0.010 [2]	0.0	0.0
B_{0040}	−0.008 (3)	0.002 [2]	0.0	0.0
A_{0050}	0.001 (3)	0.007 [2]	0.0	0.0
B_{0050}	−0.0077 (12)	−0.003 [3]	0.0	0.0
A_{0060}	0.0	0.0	−0.015 (2)	0.0
B_{0060}	0.0	0.0	0.0*	0.0

* Not refined to fix the phase origin.

Discussion

A part of the structure model (Fig. 4) was illustrated by using the computer program *PRJMS*, written by one of the authors (AY). The structure consists of columns of face-shared polyhedra, $(TiS_{6/2})_\infty$, directed along the *c* axis, with Sr atoms packed between the columns. Each column consists of domain-like linear strings of face-shared TiS_6 octahedra and Ti atoms with trigonal-prismatic coordination as domain boundaries. The atomic arrangement of a large portion of the structure somehow resembles that of the $BaNiO_3$-type structure, which is built from face-shared octahedra with the transition metal in the centre and the alkali earth located in the vicinity of the anions. The basic structure of the TiS_3 part must be composed of columns of face-shared TiS_6 trigonal prisms, because Ti and S are located at the Wyckoff positions 3(*a*) and 9(*b*) respectively of the space group *R*3*m* with $a = 11.5108$ and $c = 2.991$ Å. The real structures of TiS_3 columns and Sr rows are mutually modulated by each other, so that the S atoms are strongly twisted around the threefold axis and thus largely displaced from their basic positions. This is analogous to the situation of oxygen in $Ba_x(Cu,Pt)O_3$ analysed by Ukei, Yamamoto, Watanabe, Shishido & Fukuda (1993). In the model shown in Fig. 4, the columns of face-sharing polyhedra shift relative to each other with a basic rhombohedral symmetry and induce excess Sr sites at the adjacent positions to Ti atoms with trigonal prismatic coordination. The resulting linear density of Sr is more than one atom within the basic period of the Ti—S polyhedra.

As the two subsystems (TiS_3 and Sr) are mutually incommensurate, a description of the structure in superspace might facilitate an understanding of the subsystem relations. The modulation waves of the atomic coordinates calculated from the parameters of Table 3 are shown in Fig. 5 as functions of $t = -0.57227x_3 + x_4$. $|t|$ specifies the distance from the real three-dimensional space to the point (x_1, x_2, x_3, x_4) and hence *t* classifies the different three-dimensional space sections. The most remarkable modulation occurs in the *y* coordinate of S. In order to represent the composite crystal $Sr_{1.145}TiS_3$ in superspace, we plot the physical coordinates along c_1 and c_2, that is the *z* coordinates of the two subsystems, on the horizontal line through the origin and

the complementary coordinate t perpendicular to it, as shown in Fig. 6. Atoms Ti, S, Sr and Sr′ are depicted as wavy strings, where Sr′ is the atom obtained from Sr by the symmetry operation x, $x-y$, $\frac{1}{2}+z$ of $P31c$. In order to show the important modulations in y coordinates we express them as respective density changes of the strings in Fig. 6. A section of the four-dimensional model at an arbitrary value of t represents the real structure of the composite crystal with the corresponding phase of the modulation waves. If two neighbouring S atoms in a certain t section of Fig. 6 corresponding to, say, atoms p and q in Fig. 4 differ greatly from one another in their y coordinates, the coordination polyhedron of the Ti atom interposed between them is an octahedron. The trigonal prism of TiS_6 appears, on the other hand, when two neighbouring S atoms in the same section possess nearly equal y coordinates. This condition is satisfied at the pairs of points connected by dashed lines in Fig. 6. The equal densities of the S strings at these points show that the y coordinates are equal. While most of the TiS_6 polyhedra are octahedral, the trigonal prisms represent the minor mode of coordination. Note that the trigonal prisms appear quasi-periodically in the

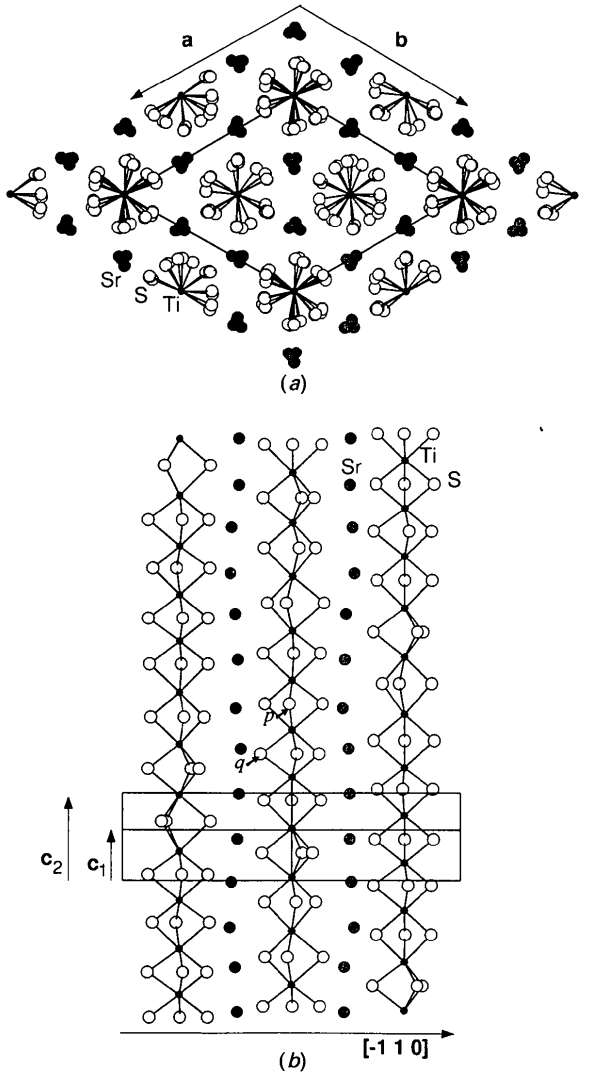

Fig. 4. (*a*) Projection of the modulated structure along [00$\bar{1}$]. (*b*) Bounded projection along [$\bar{1}\bar{1}$0]. The letters p and q indicate two neighbouring S atoms mentioned in the text. Large open, medium hatched and small solid circles represent S, Sr and Ti respectively.

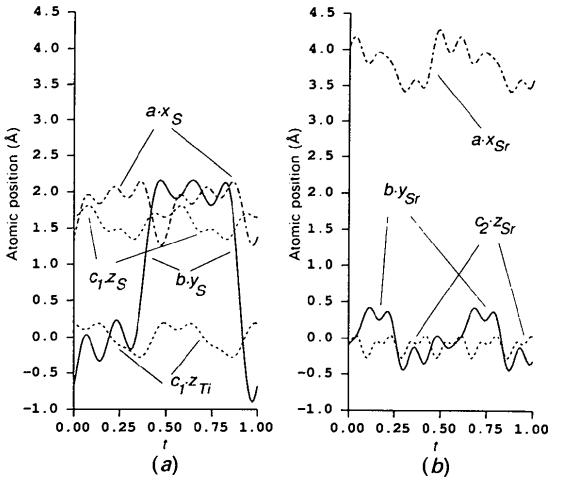

Fig. 5. Displacive modulation waves as functions of t ($=-0.57227x_3+x_4$) which classifies the different three-dimensional space section. (*a*) $a\cdot x$ and $b\cdot y$ of S, and $c_1\cdot z$ of Ti and S; (*b*) $a\cdot x$, $b\cdot y$, and $c_2\cdot z$ of Sr.

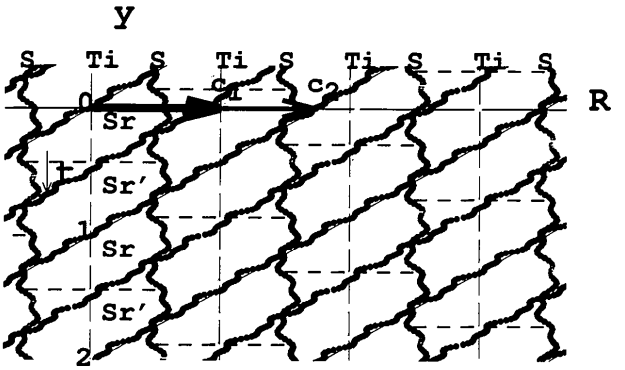

Fig. 6. Four-dimensional description of the incommensurate composite crystal $Sr_{1.145}TiS_3$. The horizontal line represents the physical coordinate along the c_1 or c_2 axis and t ($=-0.57227x_3+x_4$) is the complementary coordinate. Atoms are depicted as wavy strings with density changes corresponding to modulations in y coordinates. Sr′ is obtained from Sr by x, $x-y$, $z+\frac{1}{2}$ of $P31c$. The periodical broken lines indicate the trigonal prisms around Ti.

$(TiS_{6/2})_\infty$ chain, but strictly periodically in the superspace. Interatomic distances were calculated from the parameters of Table 3. Plots of distances of Ti—S and Sr—S are shown as functions of t in Fig. 7. The atomic parameters are modulated, in general, with a period of $\Delta t = 1$ for subsystem 1 and $\Delta t = 0.57227$ for subsystem 2. The Ti—S distances repeat themselves, however, with $\Delta t = \frac{1}{2}$. This can be explained by the fact that these atoms are situated in the special equivalent positions of $R3m$ (Table 2). The modulation function of the Ti atom includes only even-ordered Fourier components and hence has a periodicity of $\Delta t = \frac{1}{2}$. Though that of the S atom includes odd-ordered terms, their amplitudes are bound to the direction perpendicular to the mirror plane in which the Ti and S atoms are, on average, situated. Then the Ti—S distances in the first ($t = 0$ to $\frac{1}{2}$) and the second ($t = \frac{1}{2}$ to 1) half periods are the same. The striking feature of Fig. 7, that the Sr—S plots follow one after another with a phase difference of $\Delta t = 0.57227/3$, is due to the fact that the S atoms S^a S^b, S^c *etc.* are linked by the threefold screw operation. The distance for one atom pair, say Sr—S^a, remains small over the wide range because of the remarkable displacive modulation of S.

Interatomic distances and angles around some typical cases of Ti and Sr, indicated by (i), (ii), ... (vii) and (viii) in Fig. 7, are listed in Table 4(*a*) and 4(*b*) and the corresponding coordination polyhedra are illustrated in Fig. 8. The polyhedra (i)–(iv) represent (i) an almost regular octahedron, (ii) a deformed six-coordination polyhedron, (iii) a trigonal prism and (iv) an off-centred octahedron for Ti atoms. The minimum, average and maximum distances of Ti—S and the minimum distances of Sr—S are also listed in Table 4(*c*). Although the distances for Sr—S, *i.e.* the distance between two atoms each belonging to different subsystems, change in a very complicated manner in the present case because of violent displacive modulations, the coordination number of Sr may be estimated as nine for most of the crystal, as shown in Fig. 7 and Table

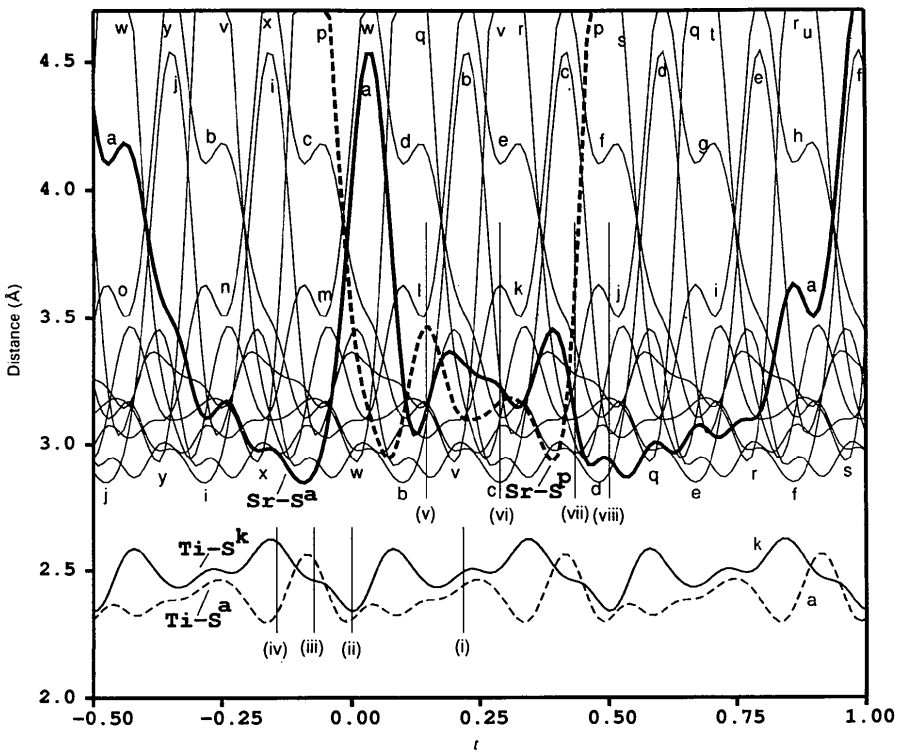

Fig. 7. Metal–sulfur distances (Å) as functions of the complementary coordinate t ($= -0.57227x_3 + x_4$). Distances equivalent to those in some typical polyhedra around Ti and Sr are designated by (i), (ii) ... and (viii). The letters, *a*, *b*, ... and *z*, represent symmetry codes of $R3m$ for S atoms as follows. (*a*) $x, y, z-1$; (*b*) $\frac{1}{3}-y, \frac{2}{3}+x-y-1, \frac{2}{3}+z-2$; (*c*) $\frac{2}{3}+y-x, \frac{1}{3}-x, \frac{1}{3}+z-2$; (*d*) $x, y, z-2$; (*e*) $\frac{1}{3}-y, \frac{2}{3}+x-y-1, \frac{2}{3}+z-3$; (*f*) $\frac{2}{3}+y-x, \frac{1}{3}-x, \frac{1}{3}+z-3$; (*g*) $x, y, z-3$; (*h*) $\frac{1}{3}-y, \frac{2}{3}+x-y-1, \frac{2}{3}+z-4$; (*i*) $\frac{2}{3}+y-x, \frac{1}{3}-x, \frac{1}{3}+z-1$; (*j*) $\frac{1}{3}-y, \frac{2}{3}+x-y-1, \frac{2}{3}+z-1$; (*k*) x, y, z; (*l*) $\frac{2}{3}+y-x, \frac{1}{3}-x, \frac{1}{3}+z$; (*m*) $\frac{1}{3}-y, \frac{2}{3}+x-y-1, \frac{2}{3}+z-1$; (*n*) $x, y, z+1$; (*o*) $\frac{2}{3}+y-x, \frac{1}{3}-x+1, \frac{1}{3}+z$; (*p*) $y-x, -x, z-1$; (*q*) $\frac{1}{3}+x, \frac{2}{3}+y-1, \frac{2}{3}+z-2$; (*r*) $\frac{2}{3}-y, \frac{1}{3}+x-y, \frac{1}{3}+z-2$; (*s*) $y-x, -x, z-2$; (*t*) $\frac{1}{3}+x, \frac{2}{3}+y-1, \frac{2}{3}+z-3$; (*u*) $\frac{2}{3}-y, \frac{1}{3}+x-y, \frac{1}{3}+z-3$; (*v*) $\frac{2}{3}-y, \frac{1}{3}+x-y, \frac{1}{3}+z-1$; (*w*) $\frac{1}{3}+x, \frac{2}{3}+y-1, \frac{2}{3}+z-1$; (*x*) $y-x, -x, z$; (*y*) $\frac{2}{3}-y, \frac{1}{3}+x-y, \frac{1}{3}+z$; (*z*) $\frac{1}{3}+x, \frac{2}{3}+y-1, \frac{2}{3}+z$.

Table 4. *Selected interatomic distances* (Å) *and angles* (°)

(*a*) Distances and angles at $t = 0$ around some typical Ti atoms shown in Figs. 7 and 8

(i)	$Ti^{(1)}$—$S^{(1)}$, $S^{(2)}$, $S^{(3)}$	2.49 (5)		$S^{(1)}$—$Ti^{(1)}$—$S^{(4)}$	92.7 (1.3)
	$Ti^{(1)}$—$S^{(4)}$, $S^{(5)}$, $S^{(6)}$	2.44 (5)		$S^{(1)}$—$Ti^{(1)}$—$S^{(5)}$	88.9 (1.8)
				$S^{(1)}$—$Ti^{(1)}$—$S^{(6)}$	175.8 (2.4)
(ii)	$Ti^{(7)}$—$S^{(7)}$, $S^{(8)}$, $S^{(9)}$	2.34 (5)		$S^{(7)}$—$Ti^{(7)}$—$S^{(10)}$	111.5 (1.9)
	$Ti^{(7)}$—$S^{(10)}$, $S^{(11)}$, $S^{(12)}$	2.30 (5)		$S^{(7)}$—$Ti^{(7)}$—$S^{(11)}$	159.6 (2.4)
				$S^{(7)}$—$Ti^{(7)}$—$S^{(12)}$	84.6 (1.8)
(iii)	$Ti^{(10)}$—$S^{(10)}$, $S^{(11)}$, $S^{(12)}$	2.46 (6)		$S^{(10)}$—$Ti^{(10)}$—$S^{(13)}$	83.4 (1.5)
	$Ti^{(10)}$—$S^{(13)}$, $S^{(14)}$, $S^{(15)}$	2.54 (6)		$S^{(10)}$—$Ti^{(10)}$—$S^{(14)}$	125.1 (5.8)
				$S^{(10)}$—$Ti^{(10)}$—$S^{(15)}$	146.0 (6.4)
(iv)	$Ti^{(13)}$—$S^{(13)}$, $S^{(14)}$, $S^{(15)}$	2.62 (5)		$S^{(13)}$—$Ti^{(13)}$—$S^{(16)}$	88.8 (1.5)
	$Ti^{(13)}$—$S^{(16)}$, $S^{(17)}$, $S^{(18)}$	2.33 (5)		$S^{(13)}$—$Ti^{(13)}$—$S^{(17)}$	95.5 (2.4)
				$S^{(13)}$—$Ti^{(13)}$—$S^{(12)}$	172.1 (2.6)

(*b*) Distances at $t = 0$ around some typical Sr atoms shown in Figs. 7 and 8

(v)	$Sr^{(48)}$—$S^{(19)}$	2.88 (4)	(vii)	$Sr^{(50)}$—$S^{(32)}$	2.98 (5)
	$Sr^{(48)}$—$S^{(20)}$	3.08 (11)		$Sr^{(50)}$—$S^{(33)}$	3.01 (7)
	$Sr^{(48)}$—$S^{(21)}$	3.14 (6)		$Sr^{(50)}$—$S^{(34)}$	3.10 (5)
	$Sr^{(48)}$—$S^{(22)}$	3.47 (6)		$Sr^{(50)}$—$S^{(35)}$	3.28 (6)
	$Sr^{(48)}$—$S^{(4)}$	3.03 (5)		$Sr^{(50)}$—$S^{(36)}$	3.25 (8)
	$Sr^{(48)}$—$S^{(23)}$	3.17 (5)		$Sr^{(50)}$—$S^{(37)}$	3.12 (11)
	$Sr^{(48)}$—$S^{(24)}$	3.15 (6)		$Sr^{(50)}$—$S^{(38)}$	3.60 (21)
	$Sr^{(48)}$—$S^{(25)}$	3.17 (5)		$Sr^{(50)}$—$S^{(31)}$	2.96 (5)
	$Sr^{(48)}$—$S^{(26)}$	3.52 (5)		$Sr^{(50)}$—$S^{(30)}$	3.40 (6)
(vi)	$Sr^{(49)}$—$S^{(27)}$	2.94 (5)	(viii)	$Sr^{(51)}$—$S^{(39)}$	2.94 (4)
	$Sr^{(49)}$—$S^{(26)}$	2.85 (4)		$Sr^{(51)}$—$S^{(40)}$	2.88 (5)
	$Sr^{(49)}$—$S^{(28)}$	3.10 (6)		$Sr^{(51)}$—$S^{(41)}$	3.05 (6)
	$Sr^{(49)}$—$S^{(29)}$	3.26 (17)		$Sr^{(51)}$—$S^{(42)}$	3.32 (7)
	$Sr^{(49)}$—$S^{(30)}$	3.07 (5)		$Sr^{(51)}$—$S^{(45)}$	3.06 (5)
	$Sr^{(49)}$—$S^{(1)}$	3.23 (4)		$Sr^{(51)}$—$S^{(43)}$	3.18 (5)
	$Sr^{(49)}$—$S^{(3)}$	3.17 (5)		$Sr^{(51)}$—$S^{(44)}$	3.17 (4)
	$Sr^{(49)}$—$S^{(4)}$	3.11 (5)		$Sr^{(51)}$—$S^{(46)}$	3.13 (5)
	$Sr^{(49)}$—$S^{(31)}$	3.63 (4)		$Sr^{(51)}$—$S^{(47)}$	3.56 (4)

(*c*) The minimum, average and maximum distances of Ti—S and the minimum distances of Sr—S

	Minimum	Average	Maximum
$Ti^{(7)}$—$S^{(7)}$	2.34 (5)	2.49 (5)	2.62 (5)
$Ti^{(7)}$—$S^{(10)}$	2.30 (6)	2.39 (5)	2.56 (5)
$Sr^{(7)}$—$S^{(10)}$	2.85 (5)		
$Sr^{(7)}$—$S^{(12)}$	2.93 (4)		

Symmetry operators: (1) $x_1, x_2, x_3 + 3, x_4$; (2) $-x_2, x_1 - x_2, x_3 + 3, x_4$; (3) $x_2 - x_1, -x_1, x_3 + 3, x_4$; (4) $x_1, x_2, x_3 + 2, x_4$; (5) $-x_2, x_1 - x_2, x_3 + 2, x_4$; (6) $x_2 - x_1, -x_1, x_3 + 2, x_4$; (7) x_1, x_2, x_3, x_4; (8) $-x_2, x_1 - x_2, x_3, x_4$; (9) $x_2 - x_1, -x_1, x_3, x_4$; (10) $x_1, x_2, x_3 - 1, x_4$; (11) $-x_2, x_1 - x_2, x_3 - 1, x_4$; (12) $x_2 - x_1, -x_1, x_3 - 1, x_4$; (13) $x_1, x_2, x_3 - 2, x_4$; (14) $-x_2, x_1 - x_2, x_3 - 2, x_4$; (15) $x_2 - x_1, -x_1, x_3 - 2, x_4$; (16) $x_1, x_2, x_3 - 3, x_4$; (17) $-x_2, x_1 - x_2, x_3 - 3, x_4$; (18) $x_2 - x_1, -x_1, x_3 - 3, x_4$; (19) $\frac{1}{3} - x_2, \frac{2}{3} + x_1 - x_2, \frac{2}{3} + x_3 + 1, x_4$; (20) $\frac{1}{3} - x_2, \frac{2}{3} + x_1 - x_2, \frac{2}{3} + x_3, x_4$; (21) $x_1, x_2, x_3 + 1, x_4$; (22) $x_2 - x_1, -x_1, x_3 + 1, x_4$; (23) $\frac{2}{3} + x_2 - x_1, \frac{1}{3} - x_1, \frac{1}{3} + x_3 + 1, x_4$; (24) $\frac{2}{3} - x_2, \frac{1}{3} + x_1 - x_2, \frac{1}{3} + x_3 + 1, x_4$; (25) $\frac{2}{3} + x_2 - x_1, \frac{1}{3} - x_1, \frac{1}{3} + x_3, x_4$; (26) $\frac{2}{3} + x_2 - x_1, \frac{1}{3} - x_1, \frac{1}{3} + x_3 + 2, x_4$; (27) $\frac{2}{3} + x_2 - x_1, \frac{1}{3} - x_1, \frac{1}{3} + x_3 + 3, x_4$; (28) $\frac{1}{3} + x_1, \frac{2}{3} + x_2, \frac{2}{3} + x_3 + 2, x_4$; (29) $\frac{1}{3} - x_2, \frac{2}{3} + x_1 - x_2, \frac{2}{3} + x_3 + 2, x_4$; (30) $\frac{1}{3} - x_2, \frac{2}{3} + x_1 - x_2, \frac{2}{3} + x_3 + 3, x_4$; (31) $x_1, x_2, x_3 + 4, x_4$; (32) $\frac{2}{3} + x_2 - x_1, \frac{1}{3} - x_1, \frac{1}{3} + x_3 + 5, x_4$; (33) $\frac{2}{3} - x_2, \frac{1}{3} + x_1 - x_2, \frac{1}{3} + x_3 + 4, x_4$; (34) $\frac{1}{3} + x_1, \frac{2}{3} + x_2, \frac{2}{3} + x_3 + 4, x_4$; (35) $\frac{1}{3} - x_2, \frac{2}{3} + x_1 - x_2, \frac{2}{3} + x_3 + 4, x_4$; (36) $\frac{1}{3} - x_2, \frac{2}{3} + x_1 - x_2, \frac{2}{3} + x_3 + 5, x_4$; (37) $x_1, x_2, x_3 + 5, x_4$; (38) $x_2 - x_1, -x_1, x_3 + 5, x_4$; (39) $1 - x_2, x_1, x_3 - 1, \frac{1}{2} + x_4$; (40) $1 - x_2, -x_1, x_3 - 2, \frac{1}{2} + x_4$; (41) $\frac{2}{3} + x_1, \frac{1}{3} + x_1 - x_2, \frac{1}{3} + x_3 - 2, \frac{1}{2} + x_4$; (42) $\frac{2}{3} + x_2 - x_1, \frac{1}{3} + x_2, \frac{1}{3} + x_3 \quad 2, \frac{1}{2} + x_4$; (43) $\frac{1}{3} - x_2 + 1, \frac{2}{3} - x_1 - 1, \frac{2}{3} + x_3 - 2, \frac{1}{2} + x_4$; (44) $\frac{1}{3} + x_2 - x_1 + 1, \frac{2}{3} + x_2 - 1, \frac{2}{3} + x_3 - 2, \frac{1}{2} + x_4$; (45) $\frac{2}{3} + x_1, \frac{1}{3} + x_1 - x_2, \frac{1}{3} + x_3 - 1, \frac{1}{2} + x_4$; (46) $\frac{1}{3} + x_2 - x_1 + 1, \frac{2}{3} + x_2 - 1, \frac{2}{3} + x_3 - 3, \frac{1}{2} + x_4$; (47) $\frac{1}{3} + x_2 - x_1 + 1, \frac{2}{3} + x_2 - 1, \frac{2}{3} + x_3 - 1, \frac{1}{2} + x_4$; (48) $x_1, x_2, x_3, x_4 + 1$; (49) $x_1, x_2, x_3, x_4 + 2$; (50) $x_1, x_2, x_3, x_4 + 3$; (51) $-x_2, 1 - x_1, x_3, \frac{1}{2} + x_4 - 1$.

4(*b*). The nine-coordination polyhedron around Sr, *i.e.* a deformed monocapped antiprism, consists mostly of two S atoms of a trigonal-prismatic or deformed Ti—S polyhedron, six S atoms belonging to two Ti—S octahedra and one S atom of an adjacent Sr—S polyhedron. Moreover it can be seen from the calculated distances between S and each metal that each S atom is surrounded mostly by two Ti and four Sr atoms. The computer programs *ATOML* and *BONDL* (Kato & Onoda, 1991*a*) were used, after correcting some errors, to calculate the three-dimensional atomic coordinates and the bond lengths, respectively.

Modulation has been introduced in the thermal parameters of S and Sr atoms being in contact with atoms belonging to the different subsystem, besides the displacive modulation. The isotropic thermal parameter of the S atom and its mean interatomic distance to two adjacent Ti and four adjacent Sr atoms are plotted as functions of t in Fig. 9. The large isotropic thermal parameter appears when the mean interatomic distance is large. The correlation of the isotropic thermal parameters and the mean interatomic distance of Sr is analogous to that of S described above. These correlations show the validity of modulation introduced in the thermal parameters, although the improvement of R_{wp} thus achieved is not large in the present case.

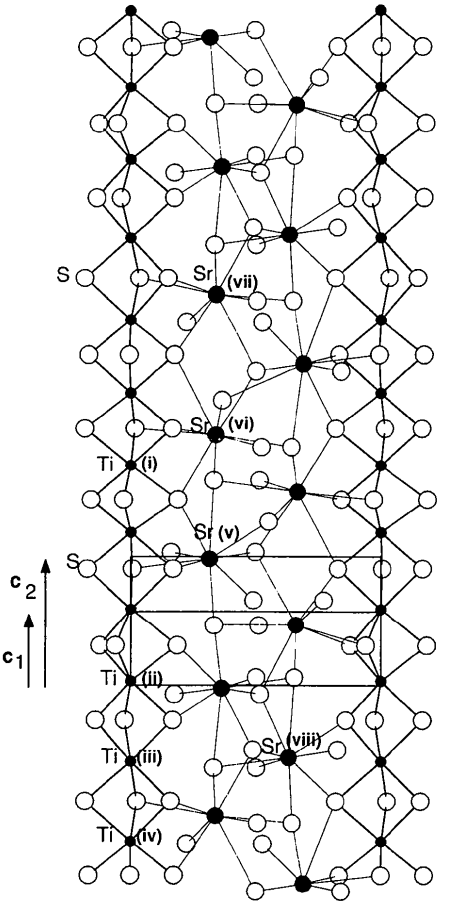

Fig. 8. Bounded projection ($-0.31 < x < 0.31$ for most atoms and $-0.36 < x < 0.36$ for some S atoms) along [$\bar{1}$00]. Coordination polyhedra around Ti and Sr listed in Table 3(*a*) and 3(*b*) are respectively indicated by (i), (ii) ... and (viii).

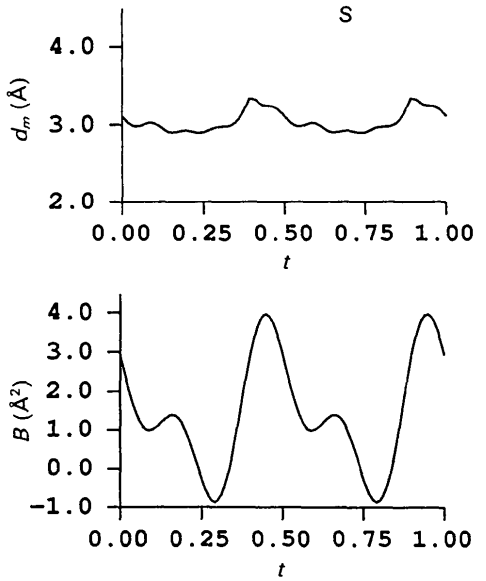

Fig. 9. The variations of the isotropic thermal parameter of the S atom and its mean interatomic distance with two adjacent Ti and four adjacent Sr atoms as functions of t ($= -0.57227x_3 + x_4$).

In this study, the crystal structure of the incommensurate composite crystal $Sr_{1.145}TiS_3$ was successfully analysed in a four-dimensional formalism using the Rietveld analysis process based on the powder X-ray diffraction data, because satellite intensities up to the sixth order were strong enough to be detected by the powder method as described above.

The authors wish to express appreciation to Mr Y. Kitami for help in electron-diffraction experiments.

References

HAHN, H. & MUTSCHKE, U. (1956). *Z. Anorg. Allg. Chem.* **288**, 269–278.
JANNER, A. & JANSSEN, T. (1980). *Acta Cryst.* A**36**, 408–415.
KATO, K. & ONODA, M. (1991*a*). *Acta Cryst.* A**47**, 55–56.
KATO, K. & ONODA, M. (1991*b*). *Acta Cryst.* A**47**, 448–449.
KATO, K. & ONODA, M. (1992). *Acta Cryst.* A**48**, 73–76.
SAEKI, M. & ONODA, M. (1993). *J. Solid State Chem.* **102**, 100–105.
UKEI, K., YAMAMOTO, A., WATANABE, Y., SHISHIDO, T. & FUKUDA, T. (1993). *Acta Cryst.* B**49**, 67–72.
YAMAMOTO, A. (1992). *Acta Cryst.* A**48**, 476–483.
YAMAMOTO, A., TAKAYAMA-MUROMACHI, E., IZUMI, F., ISHIGAKI, T. & ASANO, H. (1992). *Physica C*, **201**, 137–144.

Acta Cryst. (1993). B**49**, 936–941

Structure and Electrical Resistivity of the Heavy Fermion Compound $CeCu_5Au$

BY M. RUCK

Institut für Anorganische Chemie der Universität Karlsruhe, D-76128 Karlsruhe, Germany

AND G. PORTISCH, H. G. SCHLAGER, M. SIECK AND H. V. LÖHNEYSEN

Physikalisches Institut der Universität Karlsruhe, D-76128 Karlsruhe, Germany

(*Received* 14 *April* 1993; *accepted* 24 *May* 1993)

Abstract

The crystal structure of $CeCu_5Au$ determined at room temperature is orthorhombic with space group *Pnma* (No. 62). The lattice constants are a = 8.2455 (4), b = 5.0866 (3) and c = 10.3659 (5) Å with V = 434.76 (7) Å^3 and four formula units per unit cell. Four-circle diffractometry shows that $CeCu_5Au$ is an ordered intermetallic phase, isomorphous with $CeCu_6$, with the Au atoms exclusively occupying the Cu(2) positions of the $CeCu_6$ structure. Measurements of the electrical resistivity of $CeCu_5Au$ at low temperatures yield a residual resistivity smaller than that of single crystals of $CeCu_{5.5}Au_{0.5}$ by a factor of four, in line with the fact that $CeCu_5Au$ is a stoichiometric compound. The temperature dependence of the resistivity indicates magnetic ordering as found previously for $CeCu_{6-x}Au_x$ with $0.1 < x < 1$.

Introduction

The intermetallic compound $CeCu_6$, a heavy fermion system (Grewe & Steglich, 1991) with an extraordinarily high linear contribution to the specific heat C [$\gamma = C/T$ ($T \rightarrow 0$) = 1.67 J mol^{-1} K^{-2} (Amato, Jaccard, Flouquet *et al.*, 1987)], is one of the few examples of these systems that neither show long-range magnetic order nor become superconducting down to the lowest measuring temperatures (10 mK in this case). On the other hand, short-range magnetic intersite correlations discovered by inelastic neutron scattering (Aeppli *et al.*, 1986; Rossat-Mignod *et al.*, 1988) and confirmed through the observation of a metamagnetic-like transition in magnetization measurements (Schröder, Schlager & Löhneysen, 1992) indicate the proximity of $CeCu_6$ to magnetic order. Indeed, substitution of Cu by Au leads